ICSV14
Cairns • Australia
9-12 July, 2007

14th International Congress on Sound & Vibration

# Implementation of the Uniform Theory of Diffraction in the Phased Beam Tracing Method

Cheol-Ho Jeong, Jeong-Guon Ih

Center for Noise and Vibration Control (NoViC), Department of Mechanical Engineering
Korea Advanced Institute of Science and Technology (KAIST)
Science Town, Daejeon 305-701, Korea
ch.jeong@gmail.com; JGIH@kiast.ac.kr

## Abstract

The phased beam tracing method (PBTM), which introduces the phase information into the geometrical acoustic technique, has a definite advantage in simulating the interference of waves at medium frequencies in an enclosed space. Generally, the diffraction effect cannot be included due to the straight propagation of triangular beams. However, the diffraction should be considered in, particularly, near corners, edges, and obstacles at low frequencies. To resolve the problem, the uniform theory of diffraction (UTD) was integrated into the PBTM to predict the low frequency response near a step discontinuity. Using the UTD, we could remove the singularity in the diffraction coefficient near shadow and reflection boundaries. Single and double diffraction were included to correct the conventional PBTM results at low frequencies. The simulation showed a good agreement with previous research and the measurement. The simulation shows a good agreement with previous work and measurement. It is though that the PBTM combined with the UTD can be a fast and efficient acoustic prediction tool in an enclosure at low and mid frequencies.

## 1. INTRODUCTION

Conventional geometrical acoustics have failed to include the diffraction phenomenon because the rays or ray tubes (so called beams) should spread out straight, i.e., not bend over any obstacles or aperture. This characteristic results in the existence of zero pressure field in the shadow zone, which consequently yields the discontinuity near the shadow boundary and reflection boundary. The diffraction considerably affects the acoustic response near the corner, edges, aperture in the screen. The diffraction problem of an infinite wedge irradiated by a point source was studied by Biot and Tolstoy [1] and extended by Medwin for solving the underwater problems and noise barrier [2]. The key feature in diffraction theory is the analytical directivity functions for the edge sources. The Kirchhoff diffraction approximation based on the Huygens' principle was introduced to represent the field diffracted through an aperture. However, it is known that this approximation theory can cause an intensive computation load [3] and lead to large errors at high frequencies [4-6]. For the object or surface that has sharp edges, the Kirchhoff approximation does not provide precise diffraction estimation.

The geometrical theory of diffraction (GTD) was initially suggested by Keller [7] to explain the diffraction in the geometrical optics field. Appropriate diffraction coefficients were derived for corners, edges, and vertices of surfaces and they have been successfully adopted for electro-magnetics as well as acoustics. It has been known that the GTD is generally superior to Kirchhoff diffraction theory in both accuracy [8-10] and efficiency at high frequencies [5,7]. The shortcoming of the theory in dealing with a sharp edge problem was corrected by the GTD [7]. However, failure of the theory was found at near shadow and reflection boundaries due to singularity in the diffraction coefficient. Kouyoumjian and Pathak [11] suggested the uniform theory of diffraction (UTD) to remove such singularities. This theory shows a considerable improvement in both accuracy and efficiency over the earlier methods. It is noted that most of the researches have been focused on the perfectly conducting surface condition [5,7,11], not the realistic impedance boundary condition.

## 2. AMALGAM OF UTD INTO THE PBTM

The phased beam tracing method (PBTM) is the modified version of the beam tracing method (BTM) for mid frequency prediction [12,13]. The definite advantage of the PBTM was achieved by retaining phase information. Interference, which is usually accepted as the most predominant phenomenon at low to mid frequencies, can be described by including the phase information. In order to extend the applicability of the PBTM to low frequencies, the diffraction effect should be considered. The PBTM allows both frequency and time domain calculation. Generally, after a frequency domain response between the source and receiver is being obtained, an impulse response can be calculated by the inverse Fourier transform. In this way, the frequency domain solution for diffraction problem is more appropriate in this case.

The geometrical acoustics can predict quite accurately when the leading term of a boundary value problem is dominant compared to other higher order terms, i.e, high frequency response or weakly reverberant field. Otherwise, the higher order terms representing the wave phenomena should be taken into account to improve the precision of the simulations for general cases.

While the diffraction of half plane such as barrier or screens is the topmost problem in the outdoor propagation, the diffraction of wedge is the most important issue, in an enclosed space. One example of wedge diffraction is a step discontinuity, because there are many structures having right-angle edges such as HVAC system and furniture in a room. According to the GTD, the general expression of the diffracted pressure for spherical wave is as follows: [7,11]

$$p^d(\rho,\phi;\rho',\phi') = \frac{e^{-jk(\rho+\rho')}}{\rho'} D\left(\frac{\rho\rho'}{(\rho+\rho')},\phi,\phi'\right)\sqrt{\frac{\rho'}{\rho(\rho+\rho')}}\,. \tag{1}$$

Here, $\rho$ and $\rho'$ are the distances from the diffracted spot to receiver and source, respectively. $\phi$ and $\phi'$ are the angles from the surface to the source and receiver, respectively. Last term means a divergence factor which is the function of $\rho$ and $\rho'$.

The diffraction coefficient for the wedge of angle (2-$n$)$\pi$ [7], which is deduced by comparing the asymptotically expanded Sommerfeld's exact solution for large values of $kr$ is expressed as, if the field point is not close to a shadow or reflection boundary,

$$D_{s,h}(\phi,\phi';\beta_o) = -\frac{e^{-j\pi/4}\sin\frac{\pi}{n}}{n\sqrt{2\pi k}\sin\beta_o}\left[\left(\cos\left(\frac{\pi}{n}\right)-\cos\left(\frac{\phi-\phi'}{n}\right)\right)^{-1} \mp \left(\cos\left(\frac{\pi}{n}\right)-\cos\left(\frac{\phi+\phi'}{n}\right)\right)^{-1}\right], \tag{2}$$

where $\beta_o$ the angle between the incident ray and the tangent to the edge. In the equation, the upper sign applies to $D_s$, which is the scalar diffraction coefficient for a soft boundary and the lower to $D_h$, which stands for a hard boundary. In GTD, this expression becomes singular as the sound beam approached shadow or reflection boundaries. The regions of rapid field change adjacent to the shadow and reflection boundaries refer the transition regions. The UTD is concerned with finding proper expressions in the transition regions adjacent to shadow and reflection boundaries. The diffraction coefficient from the uniform version of the GTD for the wedge of angle (2-$n$)π can be expressed as [3,5,11]

$$D(L,\phi,\phi') = -\frac{e^{-j\pi/4}}{2n\sqrt{2\pi k}}\sum_{i=1}^{4}\cot(T_i)F(x_i), \tag{3}$$

where

$$T_{1,2} = \frac{\pi-(\phi\mp\phi')}{2n},\ T_{3,4} = \frac{\pi+(\phi\mp\phi')}{2n} \text{ and } F(x) = 2jwe^{jx^2}\int_x^\infty e^{-j\tau^2}d\tau. \tag{4}$$

Arguments of Eq. (3) are given by

$$x_{1,2} = \sqrt{\frac{2k\rho\rho'}{(\rho+\rho')}}\cos\left[\frac{2\pi nN^{\pm}-(\phi\mp\phi')}{2}\right] \text{and } x_{3,4} = \sqrt{\frac{2k\rho\rho'}{(\rho+\rho')}}\cos\left[\frac{2\pi nN^{\mp}-(\phi\mp\phi')}{2}\right]. \tag{5a,b}$$

Here, $N^+$ and $N^-$ are integers, which should almost satisfy the following relation:

$$2\pi nN^+ - [\phi\mp\phi'] = -\pi,\ 2\pi nN^- - [\phi\mp\phi'] = -\pi. \tag{6}$$

In the UTD, to resolve the singularity at the reflection/shadow boundary, Fresnel integration, $F(x_i)$ was introduced. In Eq. (3), diffraction coefficient is inversely proportional to the square root of the wave number. Consequently, the diffraction effect diminishes as the frequency becomes high.

## 3. SIMULATION RESULT

Figure 1 shows the diffraction coefficient calculated by Eq. (3). Figure 1(a) shows the perfectly conducting step in a free field. Source was located at 45° and receiver points were distributed from 0° to 270°. Figure 1(b) and 1(c) show the diffraction coefficient of the singly diffracted and doubly diffracted wave, respectively. In both figures, as the frequency goes higher, the diffraction coefficient decreases. Discontinuities in the diffraction coefficient are essential for the total field to be continuous. For single diffraction, two discontinuities, which are reflection boundary (RB) and shadow boundary (SB), respectively, are found at 135° and 225°. For doubly diffracted field, the angle of 90° is the point of discontinuity.

Zhang, et al. have studied on the acoustic pulse diffraction by 90° step and their result showed a good agreement with the previous work [14]. Diffraction pattern at $\rho=3\lambda$ from the edge of a 90° step of height $h=\lambda$ in a hard plane for essentially plane wave incidence ($\rho'=1000\lambda$, $\phi=45°$) was examined. Figure 2 shows the decomposition of sound field into two; the first pressure field is composed of the direct and specularly reflected pressure field, equivalent to the geometrical acoustics field. The second one is the pressure field by the diffraction phenomenon. The location of the source and receivers are shown in Fig. 3(a). The UTD implemented in the PBTM was compared with Zhang's result in Fig. 3(b,c). In this case, reflected sound cannot reach the observation points in the angular range from 135° to 163.1°. Therefore, the geometrical acoustics field shows discontinuity in Fig. 3(b) and diffracted portion as shown in Fig. 3(c).

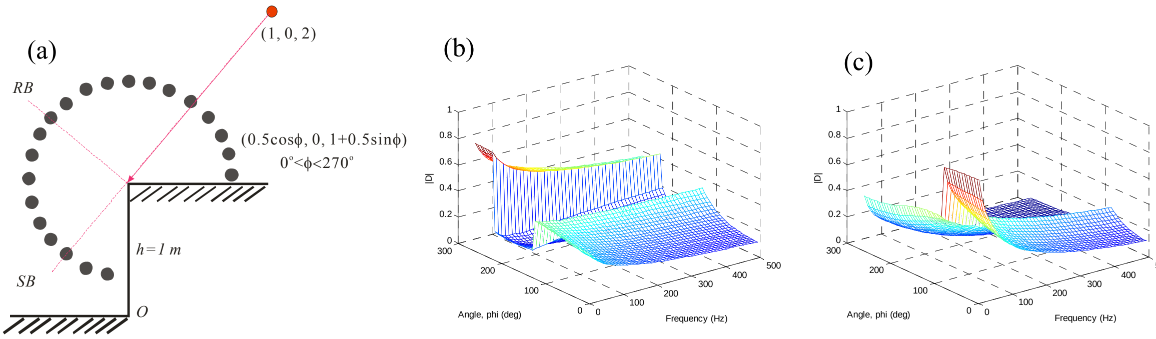


Fig. 1. Diffraction coefficient for the perfectly conducting step discontinuity. (a) 90° step model, (b) |D| for single diffraction, (c) |D| for double diffraction.

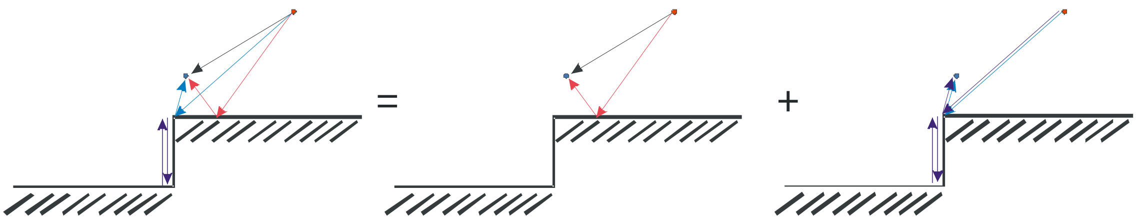

Fig. 2. Decomposition of sound paths from source to receiver.

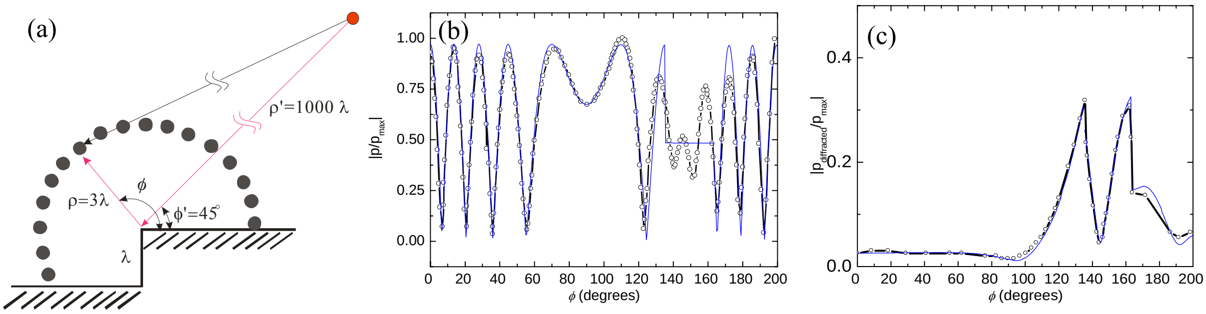


Fig. 3. Diffraction model and the pressure distribution. (a) Step model, (b) geometrical acoustics field, (c) diffracted field. —o—, Results from Ref [5]; ——, PBTM with UTD.

Figure 4 shows the pressure fields including only the single diffraction and both single and double diffractions. Single diffraction improves the simulation accuracy largely as can be seen in Fig. 4; However, there is a discontinuity at 90° due to the lack of multiple diffractions. When the double diffraction is included, the result shows excellent agreement with the previous work. From these results, it can be said that the single diffraction improves the precision of the simulation satisfactorily and the multiple diffractions plays a key role to make the pressure field continuous.

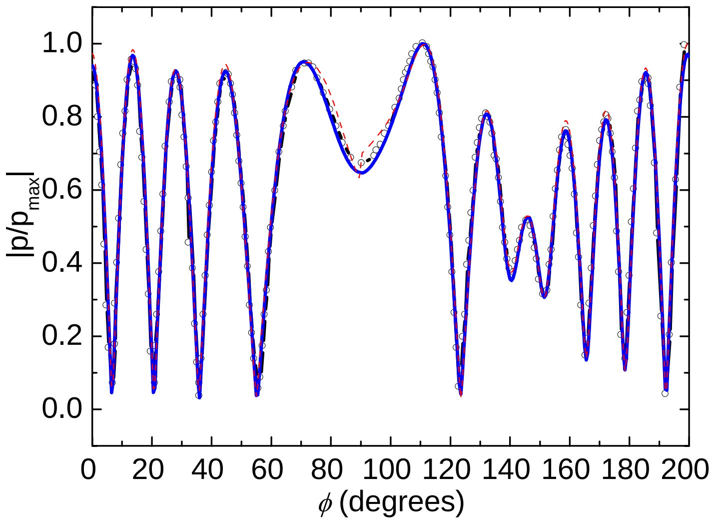


Fig. 4. A comparison of calculated pressure field. —o—, Result from Ref. [5]; ——, PBTM with total diffraction; – – –, PBTM with single diffraction.

Measurement was conducted in an anechoic chamber. As a source signal, MLS signal was employed. A dodecahedron sound source (B&K 4296) and a microphone (B&K 4130) with diffuse field corrector were used. In the first measurement, diffraction path length was shorter than the reflected path length for the step of $h$=0.68 m in Fig. 5. The locations of source and receiver were set to maximize the diffraction effect where $\phi+\phi' \approx \pi$.

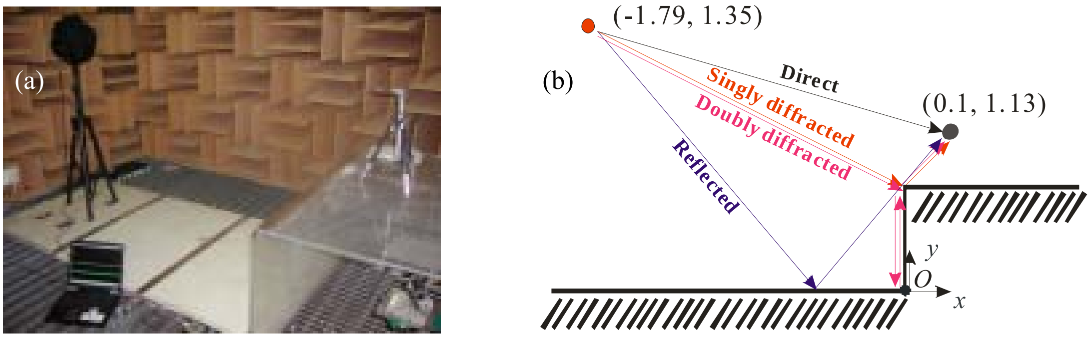


Fig. 5. Measurement setup and schematic of the experiment. (a) Photo, (b) schematic.

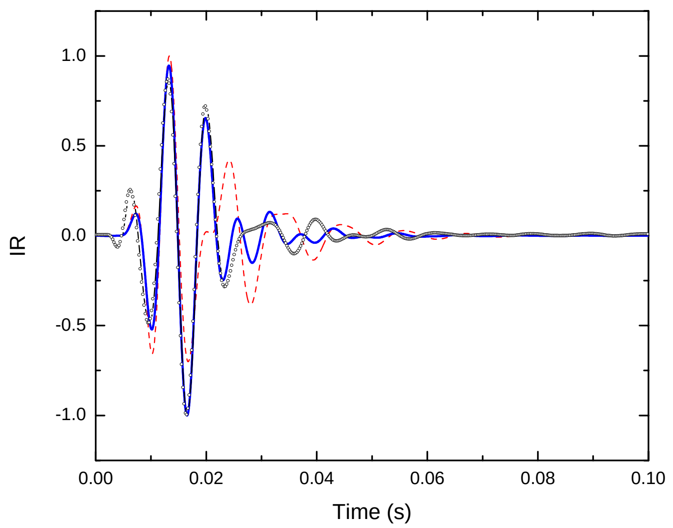


Fig. 6. A Comparison of impulse responses in 125 Hz octave band. —o—, Measurement; ——, PBTM with UTD; – – –, PBTM without diffraction.

One can find that the impulse response including diffraction effect at 125 octave band agrees better with measured data than the data obtained without diffraction correction in Fig. 6. The difference between the measurement and simulation stems from the finiteness of a step and the measurement error. The example in Fig. 7 shows the case of negligible diffraction effect, when the receiver is far from the reflection boundary. Although its influence is not appreciable, the simulation including diffraction enhances the precision of the simulation.

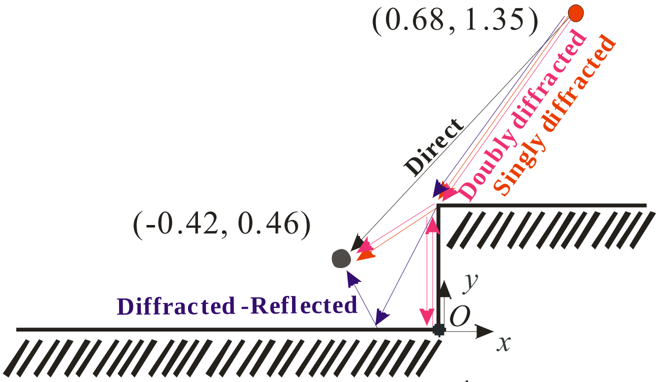


Fig. 7. Schematic drawing of the 2nd experiment.

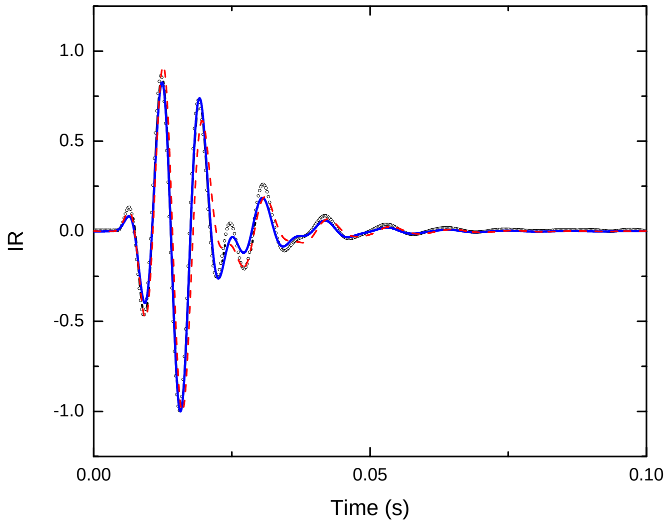


Fig. 8. A Comparison of impulse responses in 125 Hz octave band. —o—, Measurement; ——, PBTM with UTD; – – –, PBTM without diffraction.

## 4. CONCLUSIONS

In this paper, the UTD was combined with the modified geometrical acoustics technique of PBTM to extend to the low frequency range of an enclosure. The frequency domain solution of UTD for the wedge enabled the PBTM to be applicable to the low frequency acoustic analysis of an enclosed space, otherwise the technique is just confined to the mid frequency analysis. The simulated results by the present hybrid method agreed well with the previous work and measurement. This technique can be a fast and efficient predictor in the architectural acoustics field by considering the single and double diffraction from the step discontinuity.

## ACKNOWLEDGEMENT

This work was partially supported by BK21 and NRL.

## REFERENCE


[1] M. A. Biot and I. Tolstoy, "Formulation of Wave Propagation in Infinite Media by Normal Coordinates with an Application to Diffraction," *Journal of the Acoustical Society of America* **29**, 381~391 (1957).

[2] H. Medwin, "Shadowing by Finite Noise Barrier," *Journal of the Acoustical Society of America* **69**, 1060~1064 (1981).

[3] N. Tsingos, T. Funkhouser, A. Ngan and I. Carlbom, "Modeling Acoustics in Virtual Environments Using the Uniform Theory of Diffraction," *ACM SIGGRAPH*, 2001, CD-ROM.

[4] U. P. Svensson and R. I. Fred, "An Analytic Secondary Source Model of Edge Diffraction Impulse Responses," *Journal of the Acoustical Society of America* **106**, 2331~2344 (1999).

[5] Q. Zhang, E. V. Jull and M. J. Yedlin, "Acoustic Pulse Diffraction by Step Discontinuities on a Plane," *Geophysics* **55**, 749~756 (1990).

[6] G. A. Suedan and E. V. Jull, "Scalar Beam Diffraction by a Wide Circular Aperture," *Journal of the Optical Society of America* **5**, 1629-1634 (1988).

[7] J. B. Keller, "Geometrical Theory of Diffraction," *Journal of the Optical Society of America* **52**, 116-130 (1962).

[8] R. D. Spence, "A Note on the Kirchhoff Approximation in Diffraction Theory," *Journal of the Acoustical Society of America* **21**, 98~100 (1949).

[9] A. D. Pierce, *Acoustics: An Introduction to Its Physical Principles and Applications,* Acoustical Society of America, New York, 293~294, 1994.

[10] A. D. Pierce, "Diffraction of Sound around Corners and over Wide Barriers," *Journal of the Acoustical Society of America* **55**, 941~955 (1974).

[11] R. G. Kouyoumjian and P. H. Pathak, "A Uniform Geometrical Theory of Diffraction for an Edge in a Perfectly Conducting Surface," *Proc. IEEE* **62**, 1448-1461 (1974).

[12] C.-H. Jeong, J.-G. Ih and J. H. Rindel, "An Approximate Treatment of Reflection Coefficient in the Phased Beam Tracing Method for the Simulation of Enclosed Sound Fields at Medium Frequencies," *Applied Acoustics* (2007).

[13] A. Wareing and M. Hodgson, "Beam-Tracing Model for Predicting Sound Field in Rooms with Multilayer Bounding Surfaces," *Journal of the Acoustical Society of America* **118**, 2321~2331 (2005).

[14] A. J. Soares, A. J. Giarola and C. H. Conzalez, "Plane Wave Scattering by a Step Discontinuity in a Conducting Plane," *International Symposium on Antennas and Electromagnetic theory*, 1985, pp. 235~240.